International Journal of Mathematical Archive-9(3), 2018, 106-119
Available online through www.ijma.info ISSN 2229 – 5046

EFFECTS OF SLIP CONDITIONS ON MHD STAGNATION POINT FLOW OF CASSON NANOFLUID OVER A NON-LINEAR STRETCHING SHEET DUE TO POROUS MEDIA WITH SUCTION OR BLOWING

G. VASUMATHI*, J. ANAND RAO AND B. SHANKAR*****

***Research Scholar, Department of Mathematics, O.U, Hyd., India.**

****, *****Professor, Department of Mathematics, O.U, Hyd., India.**

(Received On: 28-01-18; Revised & Accepted On: 25-02-18)

ABSTRACT

T*he main aim of this paper is to theoretically investigate the steady two-dimensional electrical MHD stagnation point flow of Casson nanofluid over a non-linear stretching sheet. Problem formulation is developed in the presence of slip conditions and suction or blowing on the non-linear stretching sheet in a porous medium. The resulting governing equations are converted into a system of non-linear ODE's by applying a suitable similarity transformation and then solved numerically by using a well-known Keller Box method. The effects of different physical parameters on the velocity, temperature and concentration profiles are shown and discussed. Numerical values of local Sherwood number and Nusselt number are tabulated.*

Keywords: *Casson nanofluid; stagnation point flow; porous medium; non-linear stretching sheet; slip conditions; suction or blowing.*

INTRODUCTION

The study of non-Newtonian fluids has gained considerable attention in the last few years because of its wide range applications in engineering and industry. Several fluids exist including drilling mud, polymer solutions, paints ketchup and shampoo and so on, which do not obey Newton's law of viscosity which shows the nonlinear relationship between stress and rate of strain of these fluids. The Casson fluid model is classified as a subclass of non-Newtonian fluid, it is discovered by Casson [1] in 1959 which exhibits yield stress. If the applied shear stress is less than yield stress then the behavior of fluid is like solid, whereas it starts moving, if applied shear stress is greater than yield stress. Some common examples of Casson nanofluid are jelly, blood, honey, tomato sauce, concentration juices etc. Boundary layer flow of Casson nanofluid and Casson nanofluid flow over different geometries were considered by many authors [2-5]. Shehzad *et.al* [6] analyzed the effect of mass transfer in the MHD flow of Casson fluid over the porous stretching sheet in the presence of chemical reaction and obtained a series of solutions for resulting non-linear flow. Bhattacharya *et.al* [7] examined an exact solution of the steady boundary layer flow of Casson fluid over a stretching or shrinking sheet. Swathi Mukhopadhyay [8] studied Casson fluid flow and heat transfer over a non-linearly stretching surface. Recently Sulochana *et.al* [9] established numerical solutions of three-dimensional Casson nanofluid induced due to permeable stretching sheet in the presence of convective boundary condition. Several other studies have addressed various aspects of Casson nanofluid [10-14].

Stagnation point is a point in the flow field where the local velocity of the fluid particle is zero. The flow near stagnation point has attracted the attention of many investigators during the past several decades, in view of its wide applications such as cooling of nuclear reactors of electronic devices by fans and many hydrodynamic processes. Ishak *et.al* [15] investigated the stagnation point flow and heat transfer over a shrinking sheet in a micropolar fluid. Mahapatra *et.al* [16] analyzed about an unsteady two-dimensional flow and heat transfer of a viscous fluid near a stagnation point over a shrinking sheet in the presence of a time-dependent free stream. The steady hydromagnetic laminar stagnation point flow of an incompressible viscous fluid impinging on a permeable stretching surface with heat generation or absorption has been discussed by Attia [17]. Recently, Wubshet Ibrahim *et.al* [18] analyzed numerically by using Range Kutta fourth-order method, heat transfer characteristics of nanofluid in the presence of magnetic field near the stagnation point flow over a stretching sheet. On the other hand Kumari and *et.al* [19] analyzed the concept of the steady MHD mixed convection flow of a viscoelastic fluid in the vicinity of two-dimensional stagnation point with a magnetic field. Many investigations are there to understand the stagnation point flow of different types of fluids over a stretching sheet [20-22].

Corresponding Author: G. Vasumathi*

The study of flow and heat transfer in a porous medium has reached much attention in last few decades, due to its wide range applications in Industries and in contemporary technologies.Dulal *et.al* [23] examined the mixed convection-radiation on stagnation point flow of nanofluids over a stretching/shrinking sheet in a porous medium with heat generation and viscous dissipation. Hitesh Kumar [24] worked on the heat transfer MHD boundary layer flow through a porous medium. Gopi Chand [25] considered an unsteady stretching surface in a porous medium and explained the viscous dissipation and radiation effects on MHD flow over it. Flow through a porous medium bounded by a vertical surface in presence of hall current was explained by Sudhakar [26]. Iswar Chandra Mandal and Swathi Mukhopadhyay [27] derived the problem on heat transfer analysis for fluid flow over an exponentially stretching porous sheet with surface heat flux. Similarity solutions for unsteady boundary flow of Casson fluid induced due to stretching sheet embedded in a porous medium in the presence of first-order chemical reaction were obtained by Makanda and Shaw [28].

The boundary layer flow caused by stretching a sheet linearly or non-linearly is an important engineering problem and has several industrial applications. The heat transfer phenomenon in stretching sheet problem is very important cooling and heating are necessary factors for the quality of end product. Hayat *et.al* [29] explored the influence of thermal radiation on the two-dimensional flow of viscous and towards non-linear stretching sheet saturated in a porous medium. Anwar *et.al* [30] utilized the Buongiorno model and investigated natural convection flow of viscous fluid induced by nonlinearly stretching sheet saturated in a nanofluid. Very recently, Pal *et.al* [31] investigated the influence of thermal radiation on mixed convection flow of nanofluid caused by non-linearly stretching/shrinking sheet. Next Monica *et.al* [32] examined MHD stagnation point flow of a Casson fluid over a non-linear stretching sheet with viscous dissipation.

On the other hand, slip conditions have significant applications in various industries and are very efficient in manufacturing processes. It is a common belief that heat transfer can be increased by adding velocity slip at the boundary. Beavers and Joseph [33] were the first who used partial slip to the fluid past permeable wall. Poornima et al. [34] considered the velocity slip at the wall for Casson fluid over a porous stretching surface. The mechanism of slip condition on stagnation point flow of Casson fluid has been reported by Hayat *et.al* [35]. Ming then [36] *et.al* examined MHD mixed convection slip flow near a stagnation point on a non-linearly vertical stretching sheet. Very recently, Ramya *et.al* [37] studied on boundary layer viscous flow of nanofluids and heat transfer over a nonlinearly Isothermal stretching sheet in the presence of heat generation/ absorption and slip boundary conditions.

Suction or injection (blowing) of a fluid through the boundary surface can significantly change the flow. Generally suction tends to increase the skin friction whereas injection acts in the opposite manner. The process of suction/blowing has also its importance in many engineering activities such as in the design of thrust bearing and radial diffusers, and thermal oil recovery [38]. Suction is applied to chemical processes to remove reactants. Injection is used to add reactants, which cool the surface, prevent corrosion or scaling and reduce the drag. Shehzad *et.al* [39] examined the effects of mass transfer on the MHD flow of Casson fluid with chemical reaction and suction. Hussain *et.al* [40] studied analytical solution for suction and injection flow of a viscoplastic Casson fluid past a stretching surface in the presence of viscous dissipation. Noreen Sher Akbar *et.al* [41] examined numerical investigation of Cattaneo-Cattanneo-Christov heat flux in CNT suspended nanofluid flow over a stretching porous surface with suction and injection.

Inspired by above investigations on Casson nanofluids and its various applications, the objective of this paper is to extend and analyse the investigation of Srinivasulu *et.al* [42] to provide the solution of MHD stagnation point flow of a Casson nanofluid over a non-linear stretching sheet in a porous medium with slip conditions and suction or injection. The governing equations are solved numerically by using the Keller – Box method and the results are discussed in the physical point of view.

FORMULATION OF THE PROBLEM

The present work is on a steady two-dimensional incompressible viscous laminar flow of an electrically conducting MHD stagnation point flow of Casson nanofluid over a non-linear stretching sheet in a porous medium with suction or injection. The X-axis is taken along the fluid flow direction and Y-axis is perpendicular to it. The flow confined to $y > 0$. Two equal and opposite forces are applied along the X-axis. Keep the origin fixed, the sheet is stretched with non-linear velocity $u_w = ax^n$, where n is non-linearstretching parameter and $a > 0$, x is the coordinate measured along the stretching surface. The applied magnetic field B(x) is normal to the stretching sheet. Assuming the wall temperature T_w and nanoparticle fractions C_w are constant at the stretching surface. T_∞ and C_∞ are the ambient temperature and nanoparticle fractions.

We also assume that the rheological equation of extra stress tensor (τ) for an isotropic and incompressible flow of a casson fluid can be written as

$$\tau_{ij} = \begin{cases} 2\left[\mu_B + \frac{p_y}{\sqrt{2\pi}}\right] e_{ij}, & \pi > \pi_c \\ 2[\mu_B + \frac{p_y}{\sqrt{2\pi_c}} e_{ij}, & \pi < \pi_c \end{cases}$$

where μ_B is the plastic dynamic viscosity, and $p_y$is the yield stress of the non-Newtonian fluid, respectively. Similarly π is the product of the component of deformationrate with itself, $= e_{ij}.e_{ij}$, $e_{ij}$is the (i,j)th component of deformation rate, π_c and is the critical values of based on non Newtonian model.

Under the above conditions, the governing equations of boundary layer flow are;

$$\frac{\partial u}{\partial x} + \frac{\partial v}{\partial y} = 0 \tag{1}$$

$$u\frac{\partial u}{\partial x} + v\frac{\partial u}{\partial y} = \upsilon\left(1 + \frac{1}{\beta}\right)\frac{\partial^2 u}{\partial y^2} + U_\infty \frac{dU_\infty}{dx} - \frac{\sigma B(x)}{\rho}(u - U_\infty) - \frac{\upsilon}{k1}(u - U_\infty) \tag{2}$$

$$u\frac{\partial T}{\partial x} + v\frac{\partial T}{\partial y} = \alpha\frac{\partial^2 T}{\partial y^2} - \frac{1}{(\rho c)_f}\frac{\partial q_r}{\partial y} + \tau\left[D_B\frac{\partial C}{\partial y}\frac{\partial T}{\partial y} + \frac{D_T}{T_\infty}\left(\frac{\partial T}{\partial y}\right)^2\right] + \frac{\upsilon}{c_p}(1 + \frac{1}{\beta})(\frac{\partial u}{\partial y})^2 \tag{3}$$

$$u\frac{\partial C}{\partial x} + v\frac{\partial C}{\partial y} = D_B\frac{\partial^2 C}{\partial y^2} + \left(\frac{D_T}{T_\infty}\right)\frac{\partial^2 T}{\partial y^2} - K_r(C - C_\infty) \tag{4}$$

With the following boundary conditions are:

$$u = u_w + N_1\frac{\partial u}{\partial y}, \quad v = v_w, \quad T = T_w + N_2\frac{\partial T}{\partial y}, C = C_w + N_3\frac{\partial C}{\partial y} \quad at \;\; y = 0,$$
$$u \longrightarrow U_\infty, \;\; v = 0, \;\; T = T_\infty, C = C_\infty \quad as \;\; y \longrightarrow \infty \tag{5}$$

where x and y represent coordinate axes along the continuous surface in the direction of motion and normal to it, respectively. u and v are the velocity components along the x and y-axes, respectively, υ - kinematic viscosity, k_1 – thermal conductivity, ρ - the density of the fluid, σ - electrical conductivity, $B(x)$ – the variable magnetic field strength, B_0 - magnetic field, β - the casson parameter and a parameter defined as the ratio of effective heat capacity of the nanoparticle material to heat capacity of the fluid respectively,$(\rho c)_f$ - heat capacity of the fluid, c_p – is the specific heat at constant pressure,k_T – is the thermal diffusion ratio, q_r – the radioactive heat flux, D_B – the Brownian diffusion coefficient,D_T – the thermophoresis diffusion coefficient, α – thermal diffusivity,K_r – chemical reaction parameter, U_∞ – free stream velocity, c_s – is the concentration susceptibility, T and C – temperature and concentration inside the boundary layer, $(\rho c)_p$ - effective heat capacity of a nanoparticle, T_∞ and C_∞- are temperature and concentration far away from the sheet,

$$\alpha = (\frac{k}{(\rho c)_f}, \tau = \left(\frac{(c\rho)_p}{(c\rho)_f}\right), \; \upsilon = (\frac{\mu}{\rho_f}).$$

By using the Rosseland approximation for radiation, we write the radiative heat flux as:

$$q_r = -\frac{4\sigma^*}{3k^*}\frac{\partial T^4}{\partial y} \tag{6}$$

where k^* is the mean absorption coefficient and σ^* is the Stefan-Boltzmann constant. Since the temperature differences within the flow field are assumed to be small, and then we linearize and expand T^4 into the Taylor series aboutT_∞, which after neglecting higher order forms takes the form

$$T^4 = 4T_\infty{}^3T - 3T_\infty{}^4 \tag{7}$$

In the view of equations (6) and (7), equation (3) is reduced as,

$$u\frac{\partial T}{\partial x} + v\frac{\partial T}{\partial y} = \alpha(1 + \left(\frac{4}{3}\right).R)\frac{\partial q_r}{\partial y} + \tau\left[D_B\frac{\partial C}{\partial y}\frac{\partial T}{\partial y} + \frac{D_T}{T_\infty}\left(\frac{\partial T}{\partial y}\right)^2\right] + \frac{\upsilon}{c_p}(1 + \frac{1}{\beta})(\frac{\partial u}{\partial y})^2$$

where $R = -\frac{4\sigma^* T_\infty{}^3}{k^* K}$ is the Radiation parameter.

Similarity transformation used in this problem is:

$$u = ax^n f'(\eta), \;\; \eta = y\sqrt{\frac{a(n+1)}{2}x^{\frac{n-1}{2}}}, \;\; v = -\sqrt{\frac{av(n+1)}{2}}x^{\frac{n-1}{2}}\left[f(\eta) + \frac{n-1}{n+1}\eta f'(\eta)\right], \theta(\eta) = \frac{T - T_\infty}{T_w - T_\infty}, \;\; \phi(\eta) = \frac{C - C_\infty}{C_w - C_\infty},$$

Using the above transformations, the non-dimensional and coupled ordinary differential equations are written as

$$\left(1 + \frac{1}{\beta}\right)f''' + ff'' + \frac{2n}{n+1}\left(\lambda^2 - f'^2\right) - (M + G)f' + (M + G)\lambda = 0 \tag{8}$$

$$\left(\frac{1}{Pr}\right).\left(1 + \left(\frac{4}{3}\right).R\right)\theta'' + f\theta' + Nb.\phi'\theta' + Nt.\theta'^2 + Ec.f''^2 = 0 \tag{9}$$

$$\phi'' + Le.f\phi' + \left(\frac{Nt}{Nb}\right).\theta'' - \gamma.Le.\phi = 0 \tag{10}$$

The transformed boundary conditions

$$f(0) = S, \quad f'(0) = 1 + A.f''(0), \quad \theta(0) = 1 + B.\theta'(0), \quad \phi(0) = 1 + C.\phi'(0), \quad at\ \eta = 0,$$
$$f'(\infty) = \lambda,\ \theta(\infty) = 0,\ \phi(\infty) = 0,\ as\ \ \eta \to \infty \tag{11}$$

where, $M = \frac{2\sigma {B_0}^2}{\rho a(n+1)}$, $\lambda = \frac{c}{a}$, $G = \frac{\upsilon}{ak1.x^{2n-1}}$, $Nb = \tau \frac{D_B}{\upsilon}(C_w - C_\infty)$, $Nt = \tau \frac{D_T}{\upsilon T_\infty}(T_w - T_\infty)$, $\gamma = \frac{2K_r}{a(n+1)x^{n-1}}$,

$\Pr = \frac{\upsilon}{\alpha}$, $Le = \frac{\upsilon}{D_B}$, $A = N_1 x^{\frac{n-1}{2}}\sqrt{\frac{a(n+1)}{2\upsilon}}$, $B = N_2 x^{\frac{n-1}{2}}\sqrt{\frac{a(n+1)}{2\upsilon}}$, $C = N_3 x^{\frac{n-1}{2}}\sqrt{\frac{a(n+1)}{2\upsilon}}$,

$S = -\frac{v_w}{x^{\frac{n-1}{2}}\sqrt{\frac{av(n+1)}{2}}}$, $Ec = \frac{\upsilon}{c_p}\frac{a^2x^{2n}}{(T_w - T_\infty)}$.

where $f(\eta)$ is the dimensionless stream function, θ - the dimensionless temperature, ϕ - is the dimensionless concentration, η - the similarity variable, M – the magnetic parameter, λ - the velocity ratio parameter, Pr - the Prandtl number, Nb – Brownian motion parameter, Nt – thermophoresis parameter, G – porosity parameter, Ec – Eckert number, γ – chemical reaction parameter, Le – Lewis number, S – suction or injection parameter, A – velocity slip parameter, B – thermal slip parameter, C – solutal slip parameter.

The equation of continuity is satisfied if we choose a stream function $\psi(x, y)$ such that

$$u = \frac{\partial \psi}{\partial y}, \quad v = -\frac{\partial \psi}{\partial x}$$

Local skin friction coefficient, local result number, and local Sherwood number are important physical parameters. They defined as,

$$C_{fx} = \frac{\mu_f}{\rho {U_w}^2}\left(\frac{\partial u}{\partial y}\right)_{y=0}, \quad Nu_x = \frac{xq_w}{k(T_w - T_\infty)} = -\frac{x\left(\frac{\partial T}{\partial y}\right)_{y=0}}{K(T_w - T_\infty)}, \text{ and } Sh_x = \frac{xq_m}{D_B(C_w - C_\infty)} = -\frac{x\left(\frac{\partial C}{\partial y}\right)_{y=0}}{C_w - C_\infty}.$$

The dimensionless forms of these parameters are:

$$\sqrt{\frac{Re_x}{2}}C_{fx} = f''(0), \qquad Nu_x = -(1+R)\sqrt{\frac{Re_x}{2}}\theta'(0), \text{ and } Sh_x = -\sqrt{\frac{Re_x}{2}}\phi'(0),$$

where the surface heat flux $q_w = k\left(\frac{\partial T}{\partial y} + \frac{\partial q_r}{\partial y}\right)_{y=0}$, the surface mass flux $q_m = k\left(\frac{\partial C}{\partial y}\right)_{y=0}$ and $Re_x = \frac{U_w K}{\upsilon}$ is the Reynolds number where k is the thermal conductivity.

NUMERICAL SOLUTION

Equations (8) – (10) subjected to the boundary conditions (11) are solved numerically using finite difference method that is known as Keller box in combination with Newton's techniques.

- Reducing higher order ODEs into systems of first-order ODEs
- Writing the systems of first-order ODEs into difference equations using central differencing scheme
- Linearizing the difference equations using Newton's method and wring it in vector form
- Solving the system of equations using block elimination method

In order to solve these equations numerically, we adopt function bvp4c in Matlab software which is very efficient in using the well-known Keller box method. In accordance with the boundary layer analysis, the boundary condition at $\eta = \infty$ is replaced by $\eta = 5$, and the step size $\Delta\eta = 0.05$ is used to obtain numerical solution with four decimal place accuracy as the criterion of convergence. Obtained ordinary non-linear Equations are solved by Keller box method for boundary condition. Accuracy of this numerical method shown in Table 1 is being validated by direct comparison with the numerical results reported by T. Srinivasulu [41]. The numerical calculations of $-\theta'(0)$, and $f''(0)$ for the values of Pr, M, n, Le, S, Nb, Nt, R, λ, β, G, Ec, γ , A, B and C are shown in Table 2.

RESULTS AND DISCUSSIONS

Table-1: The comparison of values of Skin friction coefficient $-f''(0)$ and Local nusult number $-\theta'(0)$ when $Le = \beta = 1$, $Nb = Nt = Ec = 0.1$, $\lambda = 0.2$, $S = R = G = A = B = C = n = \gamma = 0$.

			Present work		Srinivasulu et. al [42]	
Pr	M	λ	$-f''(0)$	$-\theta'(0)$	$-f''(0)$	$-\theta'(0)$
1	1	0.1	0.9342	0.4939	0.9342	0.4940
2	1	0.1	0.9342	0.6990	0.9342	0.6993
3	1	0.1	0.9342	0.8362	0.9342	0.8367
1	1	0.1	0.9342	0.4939	0.9342	0.4940
1	2	0.1	1.1301	0.4479	1.1301	0.448
1	3	0.1	1.2968	0.4109	1.1301	0.411
1	1	0.5	0.5884	0.6220	0.5885	0.6222
1	1	0.9	0.1301	0.7155	0.1301	0.7160

Table-2: Computed values of skin friction coefficient, local nusult number, and Sherwood number for various values of parameters.

Pr	M	Ec	Nb	Nt	Le	β	λ	S	R	A	B	C	G	γ	$-f''(0)$	$-\theta'(0)$	$-\phi'(0)$
1 2 3	1	0.1	0.1	0.1	1	0.5	0.2	1	1	0.5	0.5	0.5	0.5	0.2	0.6118 0.7333 0.7333	0.4064 0.7043 0.9785	0.6932 0.4279 0.1724
	2 3														0.7333 0.7333	0.3990 0.3930	0.6929 0.6929
		0.5 1.0													0.7333 0.7333	0.3285 0.2311	0.7660 0.8571
			0.5 1.0												0.7333 0.7333	0.3285 0.2311	0.7660 0.8571
				0.5 1.0											0.7333 0.7333	0.3285 0.2311	0.7660 0.8571
					2 3										0.7333 0.7333	0.4046 0.4038	1.4541 2.1739
						1.0 1.5									0.7333 0.7333	0.4004 0.3976	0.6849 0.6812
							0.5 1.0								0.8333 1.0000	0.4627 0.5316	0.7153 0.7594
								2 3							0.7333 0.7333	0.6400 0.8886	1.0145 1.3619
									2 3						0.7333 0.7333	0.2862 0.2260	0.7928 0.8399
										1.0 1.5					0.6000 0.5200	0.4000 0.3945	0.6709 0.6586
											1.0 1.5				0.7333 0.7333	0.3008 0.2371	0.7637 0.8063
												1.0 1.5			0.7333 0.7333	0.4084 0.4097	0.4512 0.3060
													1.0 1.5		0.7333 0.7333	0.4004 0.3976	0.6849 0.6812
														0.8 1.2	0.7333 0.7333	0.4056 0.4053	0.9454 1.0754

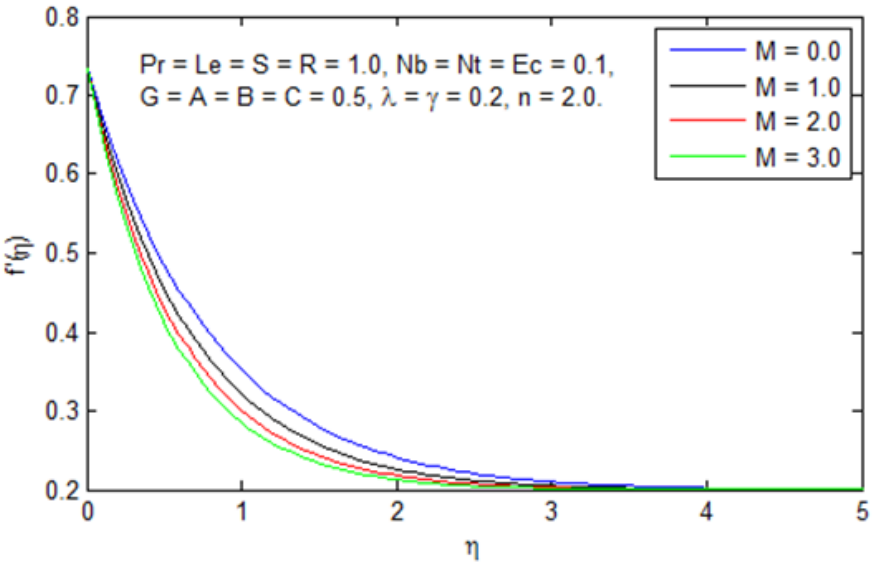

Figure-2: shows the velocity profiles for the values of M.

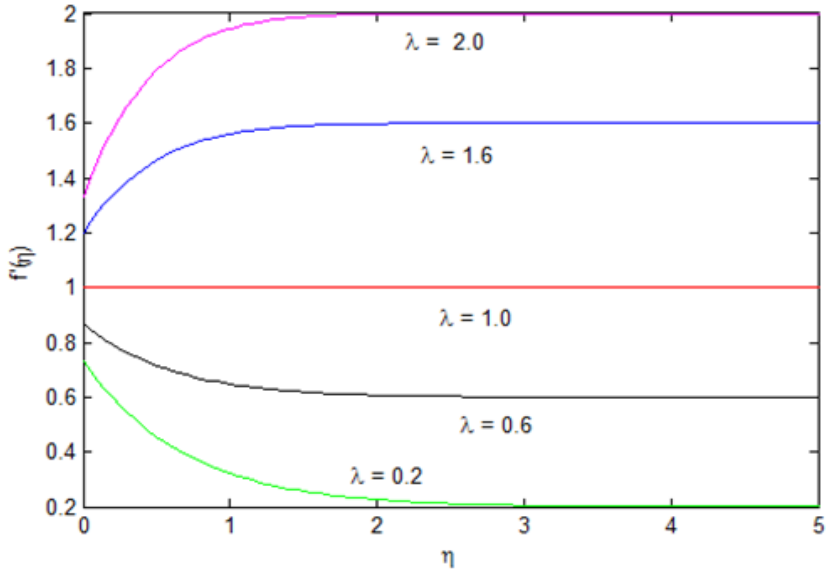

Figure-3: shows the velocity profiles for the values of λ.

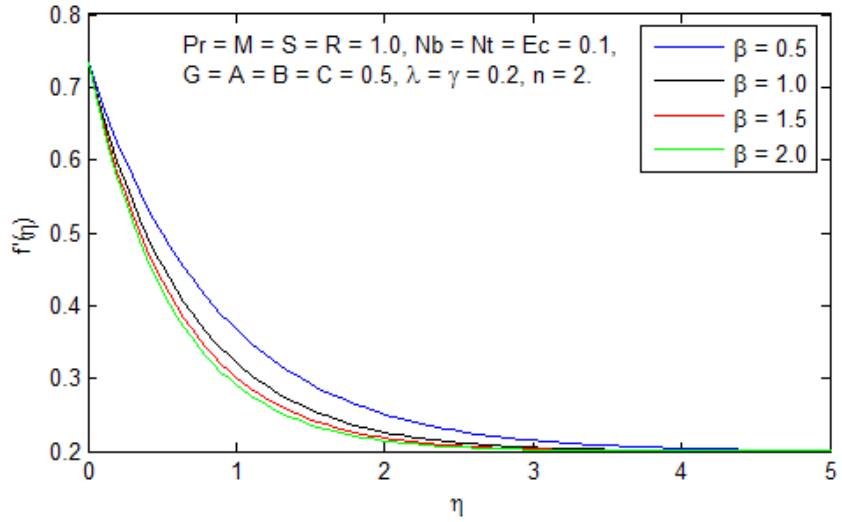

Figure-4: shows the velocity profiles for the values of β.

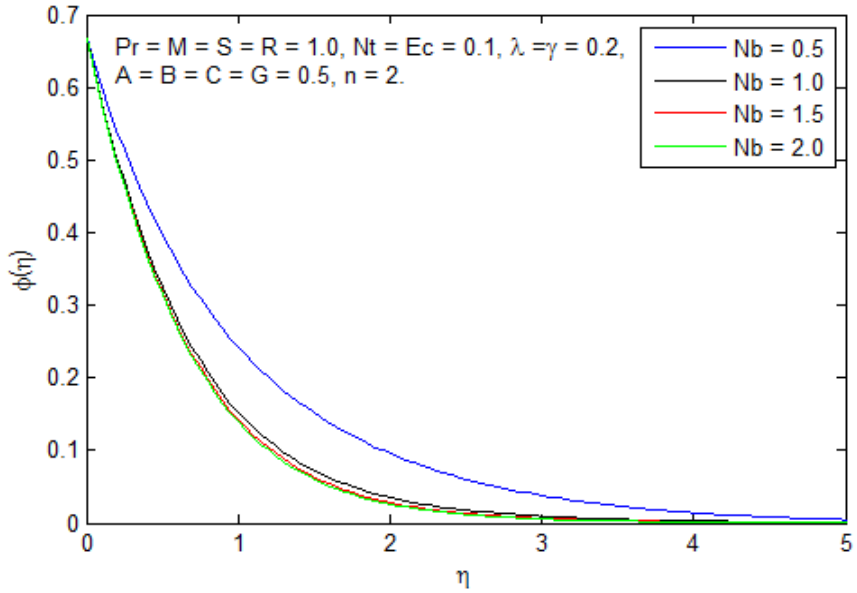

Figure-5: shows the concentration profiles for the values of Nb.

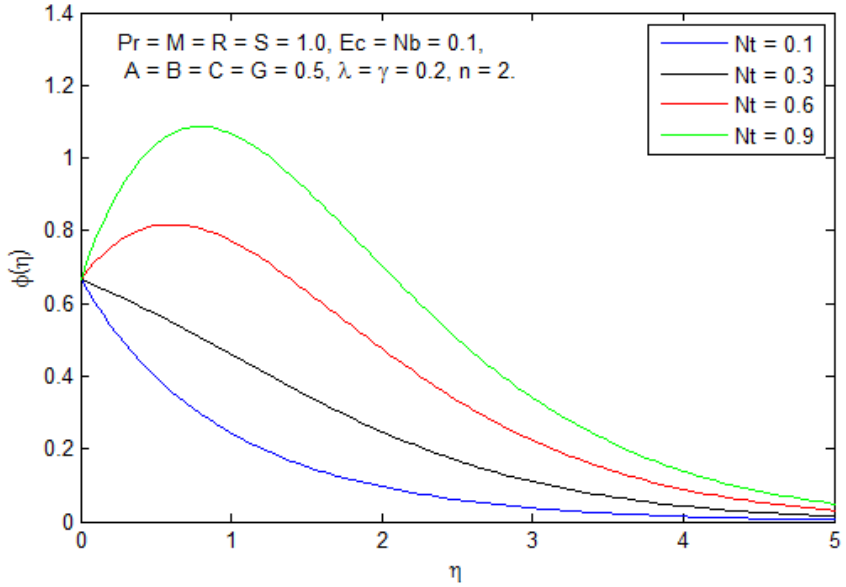

Figure-6: shows the concentration profiles for the values of Nt.

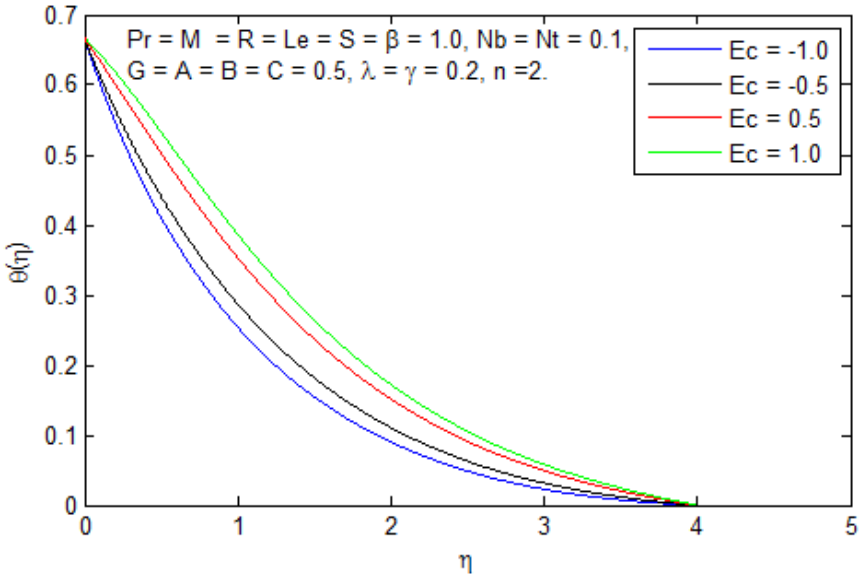

Figure-7: shows the temperature profiles for the values of Ec.

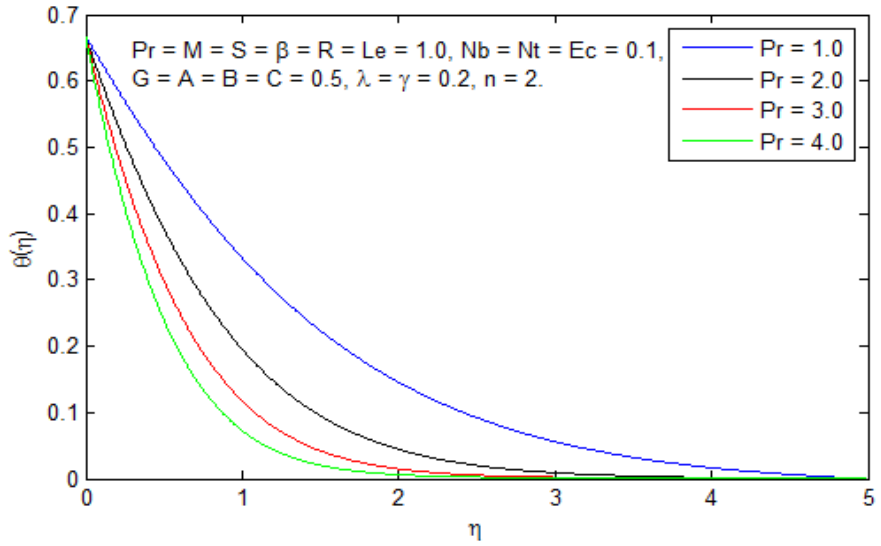

Figure-8: shows the temperature profiles for the values of Pr.

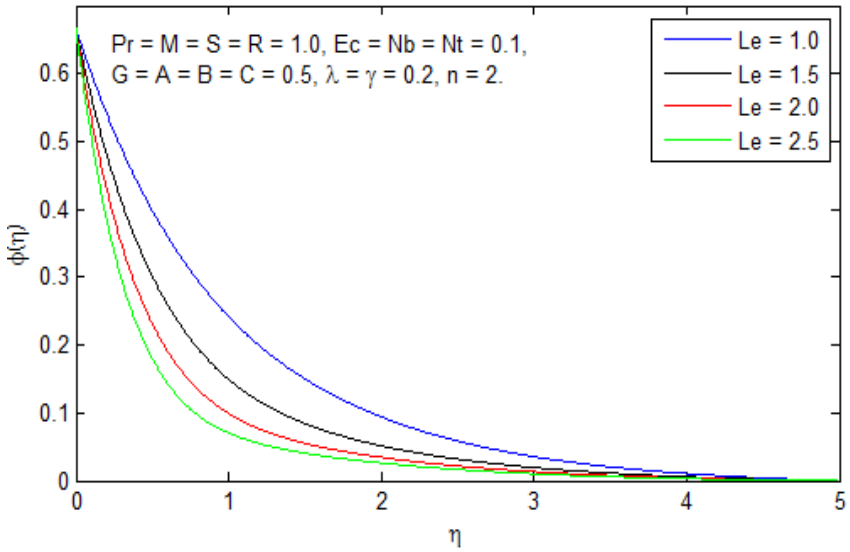

Figure-9: shows the concentration profiles for the values of Le.

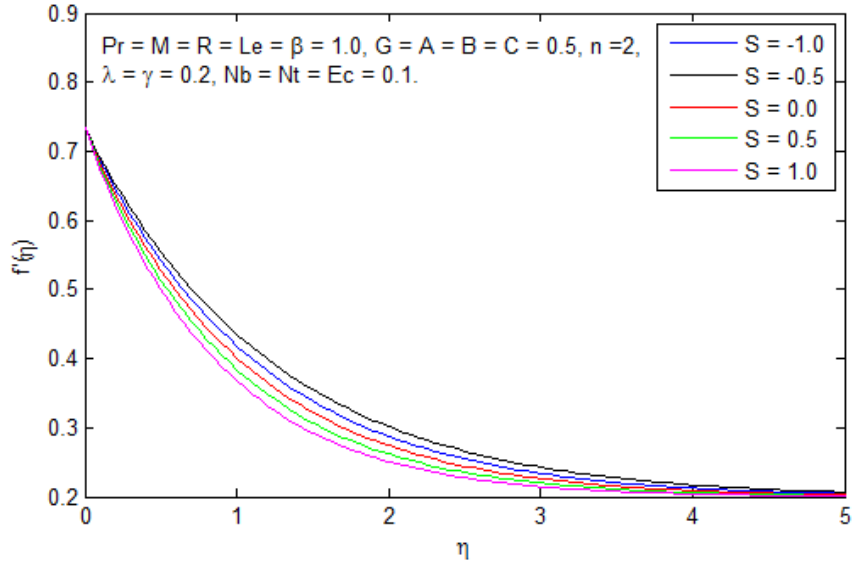

Figure-10: shows the velocity profiles for the values of S.

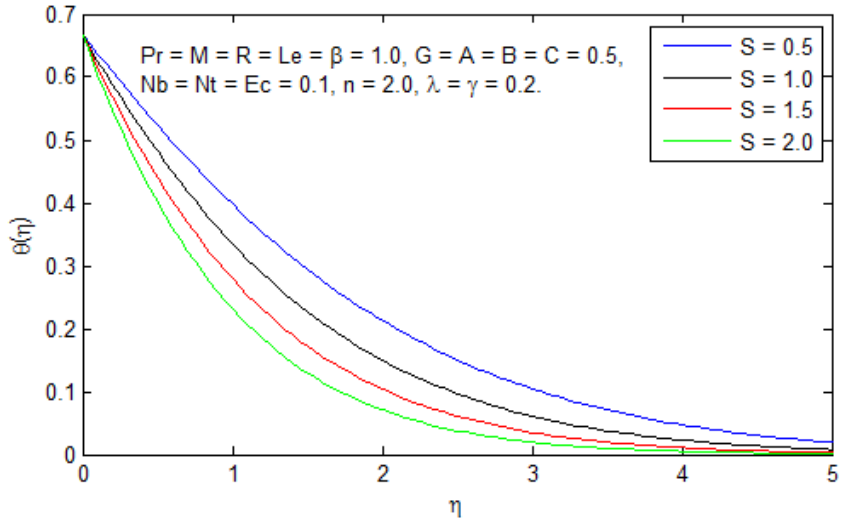

Figure-11: shows the temperature profiles for the values of S.

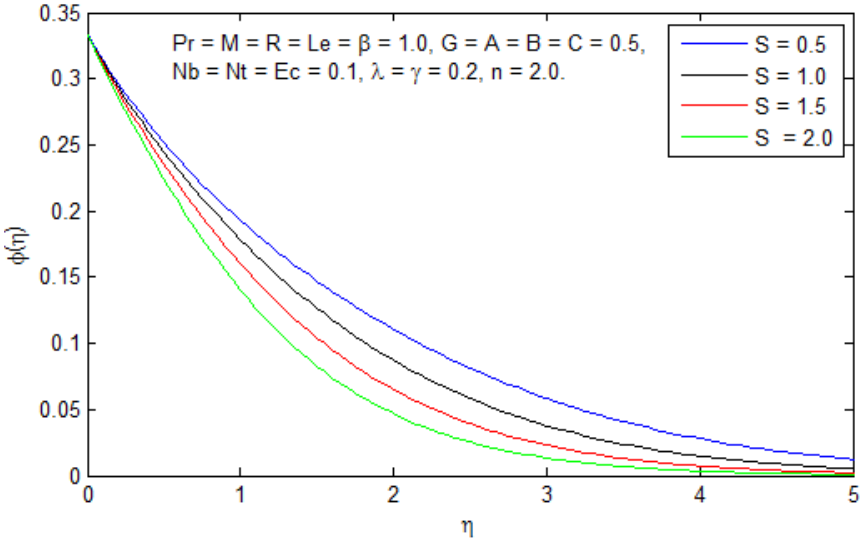

Figure-12: shows the concentration profiles for the values of S.

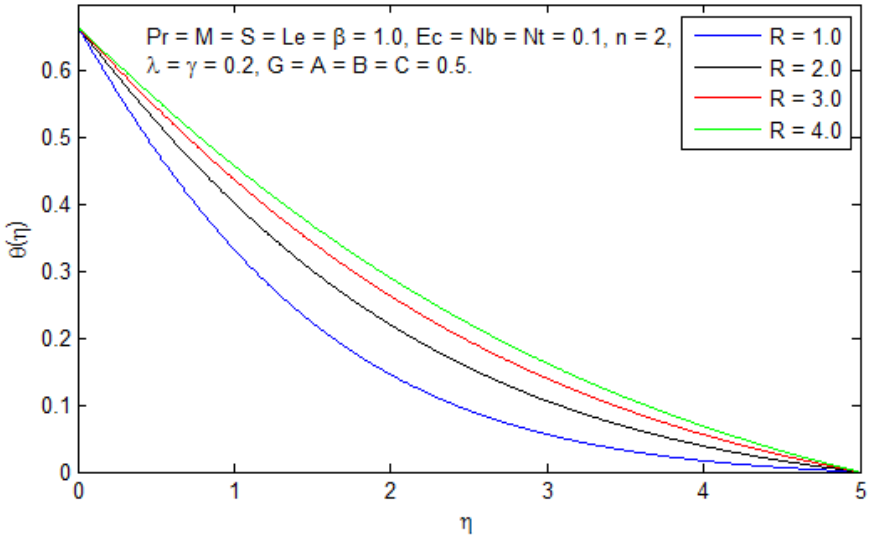

Figure-13: shows the temperature profiles for the values of R.

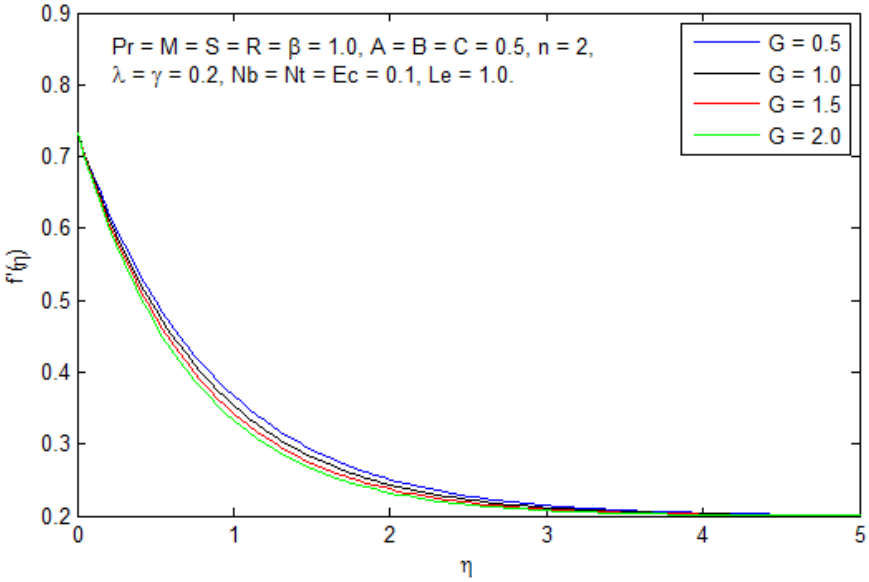

Figure-14: shows the velocity profiles for the values of G.

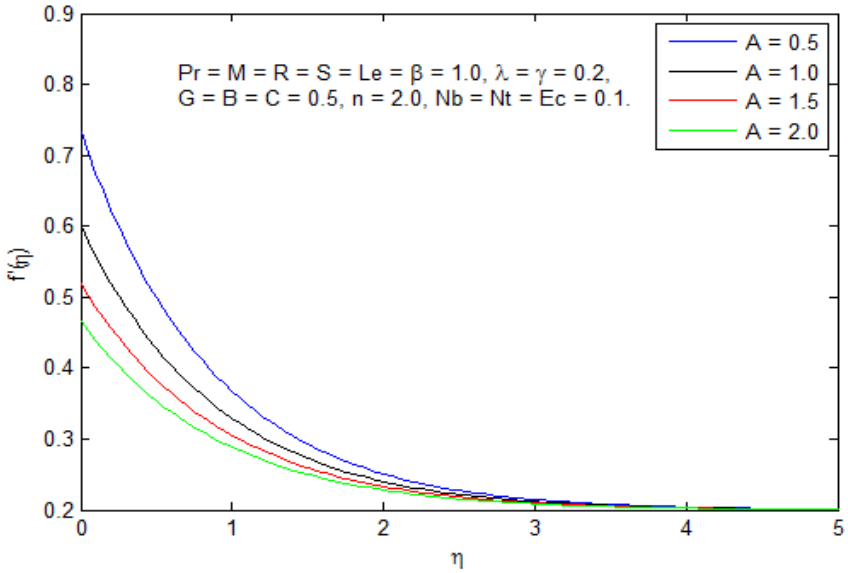

Figure-15: shows the velocity profiles for the values of A.

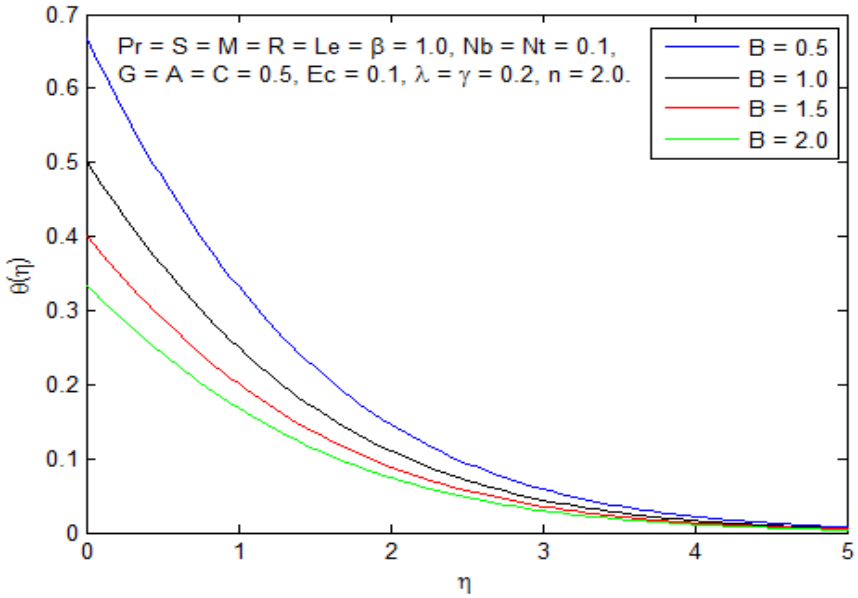

Figure-16: shows the temperature profiles for the values of B.

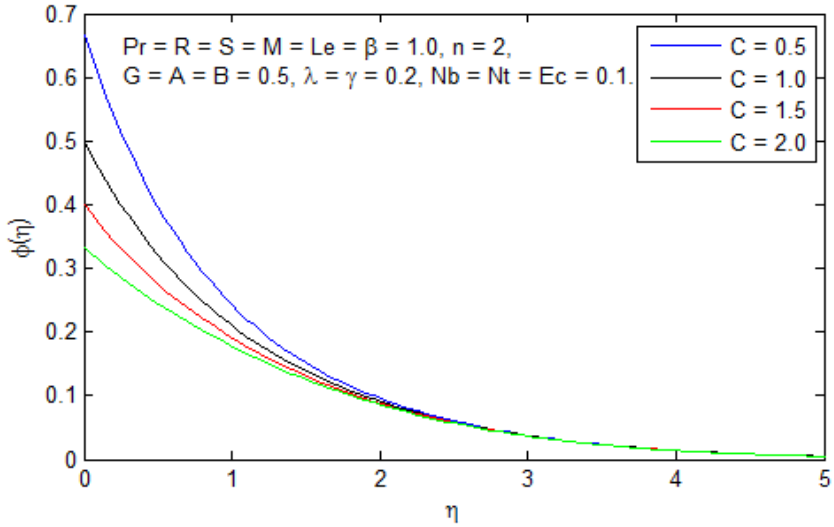

Figure-17: shows the concentration profiles for the values of C.

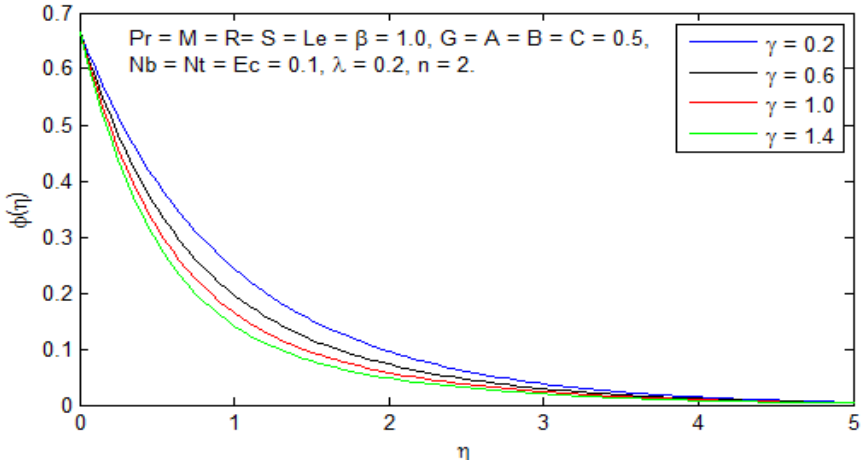

Figure-18: shows the concentration profiles for the values of γ.

Figures 2 exhibits the nature of velocity field for the variation of magnetic parameter M. With increasing M, velocity is found to decrease. As the Lorentz force opposes the motion of the fluid, much fluid is not entering to the boundary layer. It enforces the thickening of thermal layer.

Figure 3 shows the nature of velocity profiles for different values of velocity ratio parameter. When the velocity of stretching sheet exceeds the free stream velocity (i.e. $\lambda = b/a < 1$), the velocity of the fluid and boundary thickness increase with an increase in λ. When the free stream velocity exceeds the velocity of stretching sheet (i.e.$\lambda = b/a > 1$), in this case the flow velocity increases and the boundary layer thickness decreases with an increase inλ. When the velocity of stretching sheet is equal to the free stream velocity, there is no boundary layer thickness of Casson nanofluid near the sheet.

Figure 4 shows the effect of Casson parameter β on velocity graph. It is observed that for increasing values of β the velocity profile decreases.Due to increase of β,t he yield stress p_y reduces and hence the momentum boundary layer thickness decreases.

Figure 5exhibits the nature of the concentration profiles for all values of Nb considered.It is observed that nanoparticle concentration is decreasing as Nb increasing. It seems that the Brownian motion acts to warm the fluid in the boundary layer and at the same time exacerbates particle deposition away from the fluid regime to the surface which results in a decrease of the nanoparticle concentration.

Figure 6present typical profiles for concentration for various values of thermophoresis parameter (Nt). It is observed that an increase in the thermophoresis parameter (Nt) leads to increase in fluid nanoparticle concentration. Thermophoresis serves to warm the boundary layer for low values of Prandtl number (Pr) and Lewis number (Le). So, we can interpret that the rate of mass transfer decreases with increase in Nt.

Figure 7describes the effect of Eckert number on temperature profile. Temperature increases with an increase in Eckert number. The viscous dissipation produces heat due to drag between the fluid particles and this extra heat causes an increase in the initial fluid temperature.

Referring to Figure 8 a larger Prandtl number has a relatively lower thermal diffusivity. This is because Pr is defined as the ratio of kinematic viscosity to thermal diffusivity. Thus an increase in Pr reduces thermal diffusivity; it decreases the thermal boundary layer thickness. Consequently, increases the rate of heat transfer, and thereby increases the variation in the thermal characteristics. As expected, the variation in the temperature is more pronounced for smaller values of Pr than its larger values.

Figure 9 shows the effect of Le on the dimensionless concentration for fixed values of other parameters. It is observed that for larger values of Le suppress the concentration profile i.e. inhibit nanoparticle species diffusion, as observed. There will be a much greater reduction in the concentration boundary layer thickness.

The Influence of blowing (S < 0) and suction(S > 0) on typical velocity profile is shown in figure 10. As expected the opposite results are found for suction and blowing effects. That is the blowing effect enhances the fluid velocity, whereas suction effect reduces the fluid velocity near the boundary. Physically, when stronger blowing is provided, then the fluid is pushed far away from the wall. As a result of the viscosity of fluid decreases rapidly. Consequently, the fluid velocity is accelerated. This effect acts to increase maximum velocity within in the boundary layer. The same principle operates, but in the opposite direction in case of suction.

Figure 11 represents the temperature profiles for suction/blowing parameter S. It is shown that temperature decreases with increasing suction whereas it increases due to injection. The effect of suction is to make the velocity and temperature distribution more uniform within the boundary layer.

Figure 12 represents the variation of the typical concentration profile with respect to suction/injection parameter when other parameters are fixed. It is observed that when suction increases the concentration profile increases and this phenomenon is quite opposite for the effect of increasing values of blowing. Further, it is observed that, the solute boundary layer for suction is thicker than that of blowing.

As depicted in Figure 13, it is noticed that an increase in R yields an increase in the nanofluids temperature, which leads to decrease in the heat transfer rate. Thus, the radiation should be at its minimum in order to facilitate the cooling process

Figures 14 show effect of porosity parameter G on the velocity profiles. It is observed that the presence of the porous medium, the velocity profile is decreased. This is because the porous medium inhibits the fluid not to move freely through the boundary layer. This leads the flow to decrease the boundary layer thickness.

Figure15 display the profiles of velocity with respect to the variation in velocity slip parameters A. On observing the figure, the velocity decreases as the values of velocity slip parameter A increases.

Figure16describes the nature of the profiles temperature with respect to the variation in thermal slip parameters B. On observing these figures, the temperature decreases as the values of thermal slip parameter B increases.

Figure17 illustrates the variation of concentration with respect to concentration slip parameter C. As it can be seen from the graphs, the concentration profiles decrease with the values of solutal slip parameter C.

As shown in Figure 18, it is observed that the nanoparticle volume fraction decreases with increasing values of chemical reaction parameter whereas the velocity and temperature profiles are not significant with the chemical reaction parameterγ.

CONCLUSIONS

The present paper on the steady MHD stagnation point flow due to a non-linear stretching sheet with slip effects by taking heat and mass transfer, suction/blowing, Brownian motion and thermophoresis parameters, radiation parameter, porous medium into account, are analyzed. The governing equations are approximated to a system of non-linear ordinary differential equations by a similarity transformation. The self-similar equations are solved by using Keller Box method. Our results show a good agreement with the existing work in the literature.

The results are summarized as follows:

- The steady reveals that due to an increase of the magnetic field parameter reduces the fluid velocity.
- An increase in velocity ratio λ is to increase the velocity profile.
- The Casson fluid parameter decreases the fluid velocity.
- An increase in Brownian motion Nb is to decrease the nanoparticle concentration but an increase in thermophoresis parameter Nt increases the concentration.
- Prandtl number reduces the temperature.
- An increase in Lewis number Le is to decrease the fluid concentration.
- An increase in suction parameter leads the velocity, temperature and concentration profiles to decrease.
- The radiation parameter increases the fluid velocity and temperature but decreases the concentration.
- The porosity parameter G reduces the fluid velocity.
- Velocity slip parameter decreases the velocity.
- Thermal slip parameter decreases the temperature.
- Solutal slip parameter decreases concentration.
- The chemical reaction parameter γ decreases the fluid concentration.

REFERENCES

1. N. Casson, In Rheology of Dispersed System, Pergamum Press, Oxford, UK, 1959.
2. M. Mustafa, T. Hayat, I. Pop and A. Aziz, “unsteady boundary layer flow of a Casson fluid due to impulsively started moving flat plate”, Heat transfer, Asian Research, Vol.40, Issue.6, pp.563-576, 2011.
3. S.Nadheem, Rashid Mehmood, and Noreen Sher Akbar, “Optimised analytical solution for oblique flow of a Casson nanofluid with convective boundary conditions”, International Journal of thermal sciences, Vol.78, pp.90-100, 2014.

4. Gilbert Makanda, Sachin Shaw, and Precious Sibanda, "Diffusion of chemically reactive species in Casson fluid flow over an unsteady stretching surface in a porous medium in the presence of magnetic field", Mathematical problems in engineering, Vol.2015 article ID 724596, 10 pages, 2015.
5. T.Hayat, S.Asad, and A.Alsaedi, "Flow of Casson fluid with nanoparticles", Applied mathematics and mechanics, Vol.37, no.4, pp.459-470, 2016.
6. S.A. Shehzad, T.Hayat, M.Qasim and S. Asghar, "Effects of Mass Transfer on MHD Flow of Casson Fluid with Chemical Reaction and Suction", Brazilian journal of chemical engineering, Vol. 30, pp. 187-195,2013.
7. K.Bhattacharya, T.Hayat, and A.Alsaedi, "Exact solution for boundary layer flow of Casson fluid over a permeable stretching /shrinking sheet", JAMM-Journal of Applied Mathematics and Mechanics Vol. 96, pp. 522-528, 2014.
8. Swathi Mukhopadhyay, "Casson fluid flow and heat transfer over a non-linearly stretching surface", Chinese PhysicsB, Vol. 22, no. 7, 2013.
9. C.Sulochana, G.P.Ashwin Kumar, and N.Sandeep, "Similarity solution of 3D Casson nanofluid flow over a stretching sheet with corrective boundary conditions". Journal of the Nigerian Mathematical Society, Vol. 35, pp. 128-141,2016.
10. Imran Ullah, Krishnendu Bhattacharya, Sheridan Shafie and Ilyas Khan, "Unsteady MHD Mixed Convection Slip Flow of Casson Fluid over Nonlinearly Stretching Sheet Embedded in a Porous Medium with Chemical Reaction, Thermal Radiation, Heat Generation/Absorption and Convective Boundary Conditions" PLOS One, 2016.
11. P. Bala Anki Reddy, "Magnetohydrodynamic flow of a Casson fluid over an exponentially inclined permeable stretching surface with thermal radiation and chemical reaction", Ain Shams Engineering Journal, Vol. 7, Issue 2, pp. 593-602, 2016.
12. S. Nadheem, Rizwan UI Haq, Noreen Sher Akbar and Z. H. Khan, "MHD three-dimensional Casson fluid flow past a porous linearly stretching sheet", Alexandria Engineering Journal, Vol.52, Issue. 4, pp. 577-582, 2013.
13. T. Prasanna Kumar and K. Gangadhar, "Momentum and Thermal Slip Flow of MHD Casson Fluid over a Stretching Sheet with Viscous Dissipation", IJMER, pp. Vol. 5, no. 5, 25 pages, 2015.
14. G.K. Ramesh, B. C. Prasanna Kumar, B. J. Gireesha and M. M. Rashidi, "Casson Fluid Flow near the Stagnation Point over a Stretching Sheet with Variable Thickness and Radiation", Journal of Applied Fluid Mechanics, Vol. 9, No. 3, pp. 1115-1122, 2016.
15. Khairy Zaimi and Anuar Ishak, "Stagnation-Point flow and heat transfer over a non-linearly stretching/shrinking sheet in a micropolar fluid", Abstract and Applied Analysis, Vol. 2014, Article ID 261630, 6 pages, 2014.
16. Tapas Ray Mahapatra and Samir Kumar Nandy, "Slip effects on unsteady stagnation-point flow and heat transfer over a shrinking sheet", Meccanica, Vol. 48, no. 7, 2013.
17. Hazem Ali Attia, "Stagnation Point Flow towards a Stretching Surface through a Porous Medium with Heat Generation", Turkish Journal of engineering environmental science, Vol. 30, pp. 299-306, 2006.
18. WubshetIbrahim, BandariShankar, Mahantesh .M, Nandeppanava, "MHD stagnation point flow and heat transfer due to nanofluid towards a stretching sheet", International Journal of Heat and Mass Transfer, Vol.56, Issue 1-2, pp. 1-9, 2013.
19. M. Kumari and Nath, "Steady mixed convection stagnation-point flow of upper convected Maxwell fluids with the magnetic field", International Journal of Non-Linear Mechanics, Vol. 44 (10), pp. 1048-1055, 2009.
20. M. Monica, J. Sucharitha, and Ch. Kishore Kumar," Stagnation Point Flow of a Williamson Fluid over a Nonlinearly Stretching Sheet with Thermal Radiation", American Chemical Science Journal, Vol. 13(4), pp. 1-8, 2016.
21. Tariq Javed and Irfan Mustafa,"Stagnation-point flow and heattransferovera Hyperbolicstretching sheet", Heat Transfer Research, Vol. 48, Issue 9, pp.799-810, 2017.
22. Ch. Vittal, M. Chenna Krishna Reddy, and M. Monica, "Stagnation point flow of an MHD Powell-Eyring fluid over a nonlinearly stretching sheet in the presence of heat source/sink", Journal of Progressive Research in Mathematics(JPRM), Volume 8, Issue 2, pp. 1290-1300, 2016.
23. Dulal Pal, Gopinath Mandal and Kuppalapalle Vajravalu, "Mixed convection stagnation-point flow of nanofluids over a stretching/shrinking sheet in a porous medium with internal heat generation/absorption", Communications in Numerical Analysis, Vol. 2015, No.1, pp. 30-50, 2015.
24. Hitesh Kumar, "Heat transfer in MHD boundary layer flow through a porous medium, due to a non-isothermal stretching sheet, with suction, radiation and heat annihilation", Journal of Chemical Engineering Communications, Volume 200, Issue 7, pp. 895-906, 2013.
25. G. Chand and R. N.Jat, "Flow and Heat Transfer over an Unsteady Stretching Surface in a Porous Medium", Thermal Energy and Power Engineering, Vol.3, pp. 266-272, 2014.
26. Tavva. Sudhakar Reddy, O. Siva Prasad Reddy, M. C. Raju and S. V. K. Varma, "MHD free convection heat and mass transfer flow through a porous medium bounded by a vertical surface in presence of hall current", Pelagia Research Library, Advances in Applied Science Research, Vol. 3, Issue. 6, pp. 3482-3490, 2012.

27. Iswar Chandra Mandal and Swathi Mukhopadhyay, "Heat transfer analysis for fluid flow over an exponentially stretching porous sheet with surface heat flux in a porous medium", Ain Shams Engineering Journal, Volume. 4, Issue. 1, pp. 103-110, 2013.
28. Makanda. G and Shaw .S and PS, "Diffusion of chemically reactive species in Casson fluid flow over an unsteady stretching surface in a porous medium in the presence of a magnetic field", Mathematical Problems in Engineering, Vol. 3, pp. 216–221, 2014.
29. Abbas. Z and Hayat. T," Radiation effects on MHD flow in a porous space", International Journal of Heat and Mass Transfer, Vol. 51, pp. 1024–1033, 2008.
30. Anwar. M. I, Khan. I, Sheridan. S and Salleh. M. Z,"Conjugate effects of heat and mass transfer of nanofluids over a nonlinearly stretching sheet", International Journal of Physical Science, Vol. 7, pp. 4081–4092, 2012.
31. Pal. D and Mandal. G, (2014)"Influence of thermal radiation on mixed convection heat and mass transfer stagnation-point flow in nanofluids over stretching/shrinking sheet in a porous medium with the chemical reaction", Nucl. Eng. Des, Vol. 273, pp. 644–652, 2014.
32. Monica Medicare, Sucharitha Joga, and Kishore Kumar Chidem, "MHD Stagnation Point Flow of a Casson Fluid over a Nonlinearly Stretching Sheet withViscous Dissipation", American Journal of Computational Mathematics, Vol. 6, pp. 37-48, 2016.
33. Beavers. G. S and Joseph. D. D, "Boundary conditions at a naturally permeable wall", Journal of Fluid Mechanics, Vol. 30, 1967.
34. T. Hayat, M. Farooq, and A. Alsaedi, "Thermally stratified stagnation point flow of Casson fluid with slip conditions", International Journal of Numerical Methods in Heat and Fluid Flow, Vol. 25, pp. 724-748, 2015.
35. Ming Shen, Fei Wang, and Hui Chen, "MHD mixed convection slip flow near a stagnation-point on a nonlinearly vertical stretching sheet", Boundary Value Problems, Vol. 2015, 78, 2015.
36. T. Poornima, P. Srinivasulu, N.B. Reddy, "Slip flow of Casson rheological fluid under variable thermal conductivity with radiation effects", Heat Transfer Res., Vol. 44, pp. 718-737, 2014.
37. Dodda Ramya, R. Srinivasa Raju, J. Anand Rao and M. M. Rashidi, "Boundary layer Viscous Flow of Nanofluids and Heat Transfer Over a NonlinearlyIsothermal Stretching Sheet in the Presence of Heat Generation/Absorption and slip boundary Conditions", Int. J. Nanosci. Nanotechnol, Vol. 12, No. 4, pp. 251-268, 2016.
38. F. Labropulu, J.M. Dorrepaal, and O.P. Chandna, "Oblique flow impinging on a wall with suction or blowing", Acta Mech., Vol. 115, pp. 15-25, 1996.
39. S. A. Shehzad1, T. Hayat, M. Qasim and S. Asghar, "Effects of mass transfer on the MHD flow of Casson fluid with chemical reaction and suction", Brazilian Journal of Chemical Engineering, Vol. 30, No. 01, pp. 187 - 195, 2013.
40. Abid Hussain, Mohd Zuki Salleh, Ilyas Khan and Sheridan Shafie, "Analytical solution for suction and injection flow of a viscoplastic Casson fluid past a stretching surface in the presence of viscous dissipation", Neural computing and applications, pp. 1-9, 2016.
41. Noreen Sher Akbar, Dharmendra Tripathi, and Zafar Hayat Khan, "Numerical investigation of Cattaneo-Cattanneo-Christov heat flux in CNT suspended nanofluid flow over a stretching porous surface with suction and injection", American Institute of Mathematical Sciences, Vol. 11, 4, pp. 583-594, 2018.
42. T. Srinivasulu, Shankar Bandari, and Chenna. Sumalatha, "MHD Stagnation Point Flow of Casson Nanofluid over a Stretching Sheet with effect Of Viscous Dissipation", Global Journal of Pure and Applied Mathematics. ISSN 0973-1768 Volume 13, Number 8, pp. 4229-4244, 2017.

Source of support: Nil, Conflict of interest: None Declared.